Electronic driving force for stacking fault expansion in 4*H*-SiC

Walter R. L. Lambrecht and M. S. Miao
Department of Physics, Case Western Reserve University, Cleveland, Ohio 44106-7079, USA
(Received 5 January 2006; revised manuscript received 15 February 2006; published 13 April 2006)

Trapping of electrons in stacking fault (SF) interface states may lower the energy of a SF more than it costs to form the SF. This "electronic stress" driving force for SF expansion is evaluated for single and double stacking faults in 4*H*-SiC in terms of a two-dimensional free-electron density of states model based on first-principles calculations. In contrast with previous work, which claimed that the number of electrons that can be trapped in the SF is severely limited by the potential barrier arising from the space-charge region adjacent to the SF, we find that the potential barrier is strongly reduced by screening and its effect is negligible.

DOI: 10.1103/PhysRevB.73.155312 PACS number(s): 73.20.−r, 61.72.Nn

I. INTRODUCTION

Recently, there has been considerable interest in the expansion of stacking faults (SFs) in SiC polytypes. SF expansion was observed to occur in PiN diode devices under forward bias and leads to a degradation of the devices over time.[1,2] Mostly single SFs (SSFs) are observed during this process. SF growth and specifically formation of mostly double SFs (DSFs) and small 3*C*-SiC inclusions was also observed under oxidation and annealing of *n*-type SiC.[3–5] First-principles calculations by Miao *et al.*[6] and Iwata *et al.*[7–10] showed that SFs in SiC have interface states in the fundamental band gap in spite of the fact that SFs present no severe changes in the bonding. These interface states can trap electrons and degrade the current in a device.

On the other hand, the mechanism and driving force for the SF growth are still under discussion. SFs grow by motion of the partial dislocations bounding the faulted area. Dislocation motion is usually related to mechanical stress. Thus one possible explanation would be that stress fluctuations exist in the device. However, in SiC, the brittle to ductile transition occurs only above ~1050 °C and require an applied stress of order 430 MPa for yielding at this temperature.[11] Thus it is very difficult to explain a mechanical stress fluctuation driven SF growth at room temperature as occurs in devices. Ha *et al.*[12] explicitly showed that the properties of partial dislocations involved in SF expansion were inconsistent with a mechanical stress driving force. Chung *et al.*[13] also showed that mechanical stress due to doping in the epilayer in which the SF increase occurs upon annealing is incompatible with their observations of the Burger's vectors of the dislocations.

In our previous paper on this topic,[6] we proposed the possible existence of an electronic stress due to the capture of mobile carriers in the interface gap states. The principle is simply that one might gain more energy from lowering the energy of the carriers into the trap levels than it costs to form the SF. However, to evaluate this proposal, one needs to carefully examine how many states are available for trapping electrons. An important step in this direction was taken by Kuhr *et al.*[14] Besides taking into account the density of interface states, these authors argued that the trapped electrons in the quantum well state will build up a repulsive potential which will limit the number of electrons trapped and hence reduce the energy gain. As a result, they found that the growth of SSFs cannot be explained by this mechanism, while it is a possibility for DSFs simply because the DSF has a much deeper interface energy level. While this might explain why DSFs are predominantly observed in annealing experiments, it leaves open the question of the driving force in operating devices.

In the present paper, we reconsider this question using first-principles calculations, including explicitly the extra charge in the SF region. We find that the potential barrier is far smaller than one would expect on the basis of a depletion model calculation which only includes dielectric screening. This clearly is due to the self-consistent screening of the fields by the trapped carriers themselves. We find that the effect of the barrier becomes negligible and hence the proposed driving force, while much smaller for a SSF than for a DSF, may still be operative for both cases. Furthermore, we argue that in devices in operation, the calculation of Kuhr *et al.*[14] is not applicable because it is based on thermodynamic equilibrium. In a nonequilibrium case, one may think in terms of a dynamic chemical potential which may exceed the equilibrium one and hence would further enhance the electronic driving force. Additional evidence for this point of view arises from recent observations of laser excitation induced SF expansion and shrinkage.[15]

We finally point out that the present paper does not address the kinetic question of how the barriers are overcome to induced stacking fault expansion, but only why there is a net thermodynamic driving force for their expansion in the presence of free-carrier accumulation in the SF. The kinetic question is related to partial dislocation (PD) motion since the SF is surrounded by such dislocations. Ultimately, dislocations move by kink generation and migration on the dislocation. These processes were first studied computationally by Sitch *et al.*[16] and more recently with improved computational accuracy by Blumenau *et al.*[17] The motion of PDs under the influence of an electrical current in diodes were studied experimentally by Galeckas *et al.*[18] They showed that the activation energy for dislocation motion is significantly reduced in the presence of current and proposed that a nonradiative electron-hole recombination process at some defect center along the PDs is the source of the energy to overcome the energy barriers to dislocation motion. These studies were made possible by the fact that the PDs contain also radiative

recombination centers which allowed them to visualize the dislocations during diode operation by means of spectrally selective electroluminescence imaging. In a separate paper,[19] we pointed out that the energies of the radiative center and the nonradiative center identified by the studies of Galeckas *et al.*[18] add up approximately to the band gap of 4*H*-SiC. This suggests that the same defect may be responsible. That is, the electron could be first captured nonradiatively, thereby reducing the barrier for kink migration, and subsequently could radiatively recombine with the holes in the valence band and thereby make its presence visible via luminescence. We, furthermore, suggested that this defect center might be the saddle-point configuration of the kink itself based on the previous work of Sitch *et al.*[16] which found empty gap states to be present for the saddle-point configuration of a kink on a *C*-core PD. We refer the interested reader to the above papers for further discussion. While closely related, we consider it a separate issue from the one under study in this paper.

II. COMPUTATIONAL METHOD

The calculations are performed using a full potential linearized muffin-tin orbital method (FP-LMTO).[20] In this approach, the smooth part of the charge density, potential, and wave functions is represented on a real-space mesh and Poisson's equation is solved by Fourier transforms. Inside the muffin-tin spheres, the smooth parts are replaced by the actual self-consistent all-electron quantities by the usual augmentation approach. The basis set consists of muffin-tin orbitals constructed from so-called smoothed Hankel functions.[21] This allows one to use a minimal basis set of only one κ and smoothing radius per angular momentum channel without loss of accuracy. In other words, the basis functions are even more tailored to the potential than in the usual LMTO approach by appropriately shaping the envelope functions outside the spheres. To achieve high accuracy, we applied two basis functions for *s* and *p* orbitals and one basis function for the *d* orbitals. As a test of the accuracy of the approach, we calculated the energy differences between different polytypes and obtained excellent agreement with the results of Limpijumnong *et al.*[22] obtained with a far more extended basis set. The calculated polytype energies relative to 3*C* are 4.62, −2.06, −1.96, and −1.94 meV per SiC pair for 2*H*, 4*H*, 15*R*, and 6*H* polytypes in comparison with the corresponding values of 5.4, −2.4, −3.0, and −2.1 meV from the previous calculations of Limpijumnong *et al.*[22] Interestingly, the new calculations place 15*R* between 4*H* and 6*H* as expected on the basis of hexagonality. Our polytype energy difference energies also agree closely with those calculated by Iwata *et al.*[7] The Hedin-Lundquist exchange and correlation potential[23] is used in the local spin-density functional approximation.[24]

To study the single and double stacking fault in 4*H*-SiC, we utilized supercell calculations with 20 layers of Si and C pairs. To restore the periodicity without introducing a compensating second SF in the cell, we utilize rhombohedral unit cells as explained in Ref. 6. Although in any periodic arrangement, image interactions between stacking faults cannot be completely avoided, they are negligible here because the distance between the SFs in different cells are 20 SiC layers or 7.8 Å.

III. RESULTS

A. Single SF energy gain and cost analysis

First, we consider the energy cost for creating a unit of SSF. The energies of different stacking arrangements can be calculated using a generalization of the axial next-nearest-neighbor Ising (ANNNI) model,[25,26]

$$E = -\sum_{in} J_n S_i S_{i+n}, \tag{1}$$

where as usual, a pseudospin S_i is associated with each layer, such that parallel spins signify local cubic stacking and antiparallel spins signify local hexagonal stacking, J_n represents the interaction energy between *n*th nearest-neighbor layers, and the sum contains each pair of layers once. We here consider up to third nearest-neighbor layer interactions. The J_n parameters are recalculated from the polytype energy differences,[22] and found to be $J_1=1.70$ meV, $J_2=-2.19$ meV, and $J_3=-0.42$ meV. These agree well with the values reported by Iwata *et al.*[7] We recall that using the ANNNI model,[6,22] the formation energy of a SSF in 4*H*-SiC is $-4J_2$ which is 8.8 meV per SiC formula unit using the current J_n values and is 1 meV smaller than our previous result.[6] Next, we calculate the energy gain. The latter is based on the fact that an interface state forms in the SF. To accurately determine the position of this interface band, we need the valence-band alignment. This is done by aligning the local potentials of the system with SF with the pure 4*H* SiC. It gives a valence-band offset (VBO) of type II, given by $E_v(4H)-E_v(4H-SF)=0.056$ eV. Having thus located the bulk conduction-band minimum, we obtain the maximum depth of the interface band at the *M* point to be $E_i=E_c-0.266$ eV.

We now have to consider how many states are available per pair of atoms and what their contribution is to the energy if filled with electrons trapped from the conduction band. The interface band can be well described as a parabolic band with effective masses m_1 and m_2 in the $M-\Gamma$ and $M-K$ direction, respectively. The constant energy surface thus consists of six half ellipses within the first Brillouin zone (BZ). The number of states below energy *E*, $n(E)$, and density of states function $g(E)$ are given by

$$n(E) = \frac{3A}{\pi\hbar^2}\sqrt{m_1 m_2}E\theta(E-E_i),$$

$$g(E) = \frac{3A}{\pi\hbar^2}\sqrt{m_1 m_2}\theta(E-E_i), \tag{2}$$

where E_i is the lowest energy of the interface band, θ is the step function, and *A* is the unit-cell area. The effective masses of the interface state were calculated to be $m_{MK}=0.22m_e$, $m_{M\Gamma}=0.68m_e$ close to those of the corresponding conduction-band minimum of 4*H*[27] and lead to an effective

density of states mass $m_* = \sqrt{m_1 m_2} \approx 0.39 m_e$. We note that our effective masses also agree well with those reported by Iwata *et al.*[9] This gives about 0.1 states/unit-cell area (or 1.2×10^{14} e/cm^2) below the conduction-band minimum. The contribution to the energy gain from trapping electrons in these states is given by

$$E_g = \int_{E_i}^{E_F} Eg(E)dE = \frac{3A}{2\pi\hbar^2}\sqrt{m_1 m_2}(E_F - E_i)^2. \quad (3)$$

Assuming that the Fermi level is at the CBM, this gives 14 meV. In fact, for a typical carrier density of $n = 3 \times 10^{19}$ cm^{-3}, the Fermi energy, given by the three-dimensional (3D) equation

$$n = \left(\frac{2E_F}{\hbar^2}\right)^{3/2} \sqrt{m_1 m_2 m_3}/\pi^2, \quad (4)$$

would lie 46 meV above the conduction-band minimum and the corresponding energy gain in the interface band becomes about 19 meV. In conclusion, there is a net energy gain in forming the SF of ~10 meV/pair if it can trap electrons while forming the defect. This is of course a small energy, and thus we cannot completely exclude that effects beyond the present model would further reduce it. One might have preferred a direct calculation of the Kohn-Sham density-functional total-energy difference instead of our present calculation which only includes the sum of occupied one-electron energies. However, the additional electrostatic double-counting and exchange correlation terms should be even smaller since the electrostatic potential due to the charge accumulation itself will be shown to be negligible due to screening in Sec. III C.

B. Double stacking fault

The single SF in 4*H*-SiC we discussed so far consists of a band of three cubically stacked layers whereas in 4*H*-SiC only bands of width 2 occur. Using the usual spin notation, see, for instance, Ref. 6, the 4*H*-SiC unit cell corresponds to ↑↑↓↓. The SF is produced by a slip of one layer as illustrated in Fig. 1. As already pointed out by Liu *et al.*[5] a second slip in the adjacent layer leads to a DSF with six parallel spin layers. The band structure for the DSF is shown in Fig. 2 and is consistent with earlier calculations by Iwata *et al.*[7]

It shows the existence of two interface states below the conduction band, the first of which is considerably deeper than before, at 0.68 eV below the CBM. The effective masses of this band are $m_{MK} = 0.22 m_e$ and $m_{M\Gamma} = 0.57 m_e$, giving an effective $\sqrt{m_1 m_2} = 0.35 m_e$. A second interface band is just about to emerge from the conduction band. These results are semiquantitatively explained in terms of quantum well quantum confinement. Since 3*C* has a smaller band gap than 4*H* by about 0.8 eV and the valence-band offset is quite small (<0.06 eV),[28] the conduction-band offset provides a potential well for conduction electrons. As is well known, the confinement energy for a particle in a box varies as L^{-2} with L the size of the box. Thus since the well is two times larger we expect the confinement energy to be four times smaller in the double than in the single SF. Since for the SF, the interface state occurs at 0.27 below the 4*H* conduction band, it lies 0.53 eV above the 3*C*-SiC quantum well bottom. So, we expect the interface state to lie at 0.55/4=0.13 eV above the quantum well bottom or at about 0.67 eV in agreement with the first-principles results. It should be pointed out that there is an additional spontaneous polarization effect which tilts the potential but calculations show that in the present case this field is smaller than 0.04 eV/6 layers and has only a negligible effect on the quantum well states. The screening of the spontaneous polarization was emphasized in a previous study.[29,30] The real quantum well is of course of finite depth and this will also affect the results slightly. A more detailed analysis is provided by Lindefelt *et al.*[10]

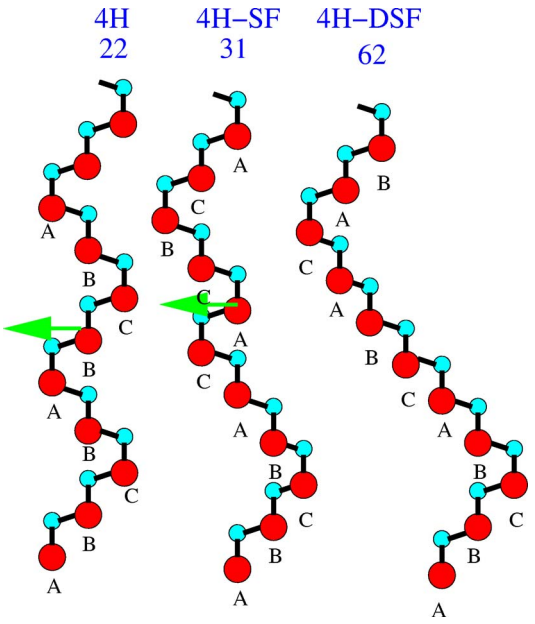

FIG. 1. (Color online) Stacking arrangements for (a) 4*H*-SiC, (b) single stacking fault, and (c) double stacking fault obtained by successive slips of one layer.

In any case, we can now repeat the calculation for the energy gain associated with capturing electrons in these interface states. Assuming again that maximum number of electrons are trapped, the energy gain is now about 83 meV

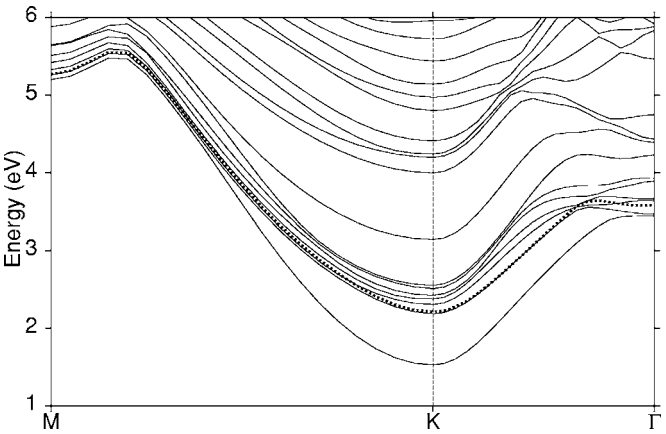

FIG. 2. Band structure of double stacking fault near conduction-band minimum of 4*H*-SiC (shown by the dotted line).

while the energy cost of forming the 2SF within the ANNNI model is only $-4(J_1+2J_2)=10.7$ meV. Thus a substantially larger energy gain occurs in this case. We emphasize that the extra energy cost of forming a DSF once a SSF already exists is very small (1.96 meV/SiC pair) and, more importantly, the gain by trapping electrons is substantially larger, leading to about an order of magnitude larger net energy gain for forming the DSF. The results on the neutral interface energy of formation of the SSF and DSF agree well with the calculations by Iwata *et al.*[7,8]

Interpreting the energy gain per unit area as a force on the surrounding dislocation line, or an outward pressure tending to expand the faulted area, we note that 10 meV/unit cell area corresponds to a force of 0.02 N/m for the SF. For the DSF we obtain 79 meV/pair or 0.15 N/m. Dividing this by the size of a Burger's vector $(a/\sqrt{6})$ one arrives at a stress of the order of ~100 MPa for a SF and ~850 MPa for the DSF. These are considerable stresses comparable to the yield stresses[11] which could easily dominate mechanical stress fluctuations.

C. Potential barrier effect

Thus far, we have included the effect of the density of available states but not yet the self-consistent re-arrangement of the charge density around the SF or the finite temperature. Following the discussion of Kuhr *et al.*[14] one needs to take into account the potential barrier that results from the space-charge region surrounding the SF on both sides. While they carried this calculation out including a temperature-dependent Fermi distribution, we can easily reproduce their results with the following simplified calculation at zero temperature. The potential barrier in the depletion region is given by $V=2\pi N_d L^2/\kappa$ with L the width of the depletion region, κ the dielectric constant, N_d the donor concentration, and using atomic units. Charge neutrality requires that the electron charge in the SF, treated as a 2D sheet of charge with surface density σ be compensated by the donor charge in the two depletion layers, thus $\sigma=2N_dL=\sqrt{2\kappa V N_d/\pi}$. On the other hand, raising the SF energy means that the interface band is replaced by E_i+V, thus the first of Eqs. (2) becomes $\sigma=(3m_*/\pi\hbar^2)(E_F-E_i-V)$. Solving these two equations for σ yields a quadratic equation for V which gives

$$V=(E_F-E_i)+\frac{\alpha}{2}\sqrt{(E_F-E_i)\alpha+\frac{\alpha^2}{4}}, \tag{5}$$

with $\alpha=2\pi\kappa N_d/(3m_*)^2$. This calculation does not include the temperature effect but even at elevated temperatures, the Fermi function can be approximately treated as a step function, as we did implicitly in Eq. (2). Plugging in some typical values, such as $N_d=10^{19}$ cm^{-3}, gives a $V=244$ meV with $\sigma=1.1\times10^{13}e/\text{cm}^2$ giving $E_g=0.1$ meV. Even for as high as $N_d=10^{20}$ cm^{-3}, $V=197$ meV, $\sigma=3.4\times10^{13}e/\text{cm}^2$, and $E_g=0.9$ meV the gain is still negligible. Kuhr *et al.*[14] further studied the temperature and doping level dependence of this effect in detail. With increasing temperature and doping level, the barrier becomes reduced. Nevertheless, the result of this model is that no net electronic driving force remains in effect for a SSF. For the DSF, the barrier potential is similar but the interface state is significantly deeper, 0.68 eV, and thus a net driving force remains.

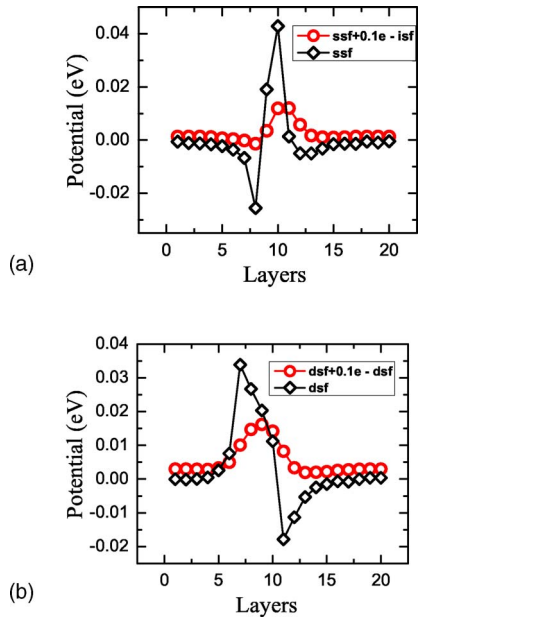

FIG. 3. (Color online) Profile of the average potentials at the Si muffin-tin spheres for SSF (top panel) and for DSF (bottom panel). To filter out the oscillation of the 4*H* potential profile, we show the running average between two adjacent layers (black diamonds). The line with the red circles shows the differences between the potentials of the SSF and DSF with and without the extra $0.1e$/unit cell charges.

The above model of the barrier formation, however, rests on the depletion approximation. It is assumed that the SF is negligibly thin compared to the space-charge region and can be represented by a strictly two-dimensional sheet of charge. In reality if the width of the SF itself is considered, the potential will not be purely parabolic anymore but will be rounded off near the top and hence the model gives an overestimate of the effect. More importantly, the model includes only dielectric screening in the space-charge region. However, with a carrier concentration of order 10^{19} cm^{-3} metallic type screening cannot be neglected. In fact, this corresponds to a Thomas-Fermi screening length of 2.5 Å. Thus we expect significant screening over short distances near the SF rather than dielectric screening over a wide space-charge region.

To investigate this effect quantitatively, we set up calculations on SSF and DSF systems with an extra charge density of $0.1e$/unit cell, which is about 2.4×10^{20} cm^{-3}. Charge neutrality is maintained by adding an opposite uniform background charge. We found that the state localized at the SF shifts up by only 2 meV, much less than the depletion model predicts. Apparently this small shift of the SF level will not affect the mechanism of electron trapping. To gain further insight, we plot the potential profile of the SSF and DSF in Fig. 3. These potential profiles show the average potential on Si muffin-tin sphere radii, filtered so as to maintain only the slowly varying part of the potential by taking a running average over two subsequent (cubic or hexagonal) layers in the direction perpendicular to the layers. The potentials without

extra charge (indicated by black diamonds) clearly show the effect of spontaneous polarization manifesting itself in an approximately linear potential inside the QW. Note, however, that in the barrier region the potential goes back to a constant value within a few layers, rather than being a straight zigzag line as a straightforward spontaneous polarization model would predict. This point was emphasized earlier in Refs. 29 and 30. The second curve (red circles) shows the change induced by adding the extra electrons explicitly in the system. While one indeed sees a rise in potential in the SF region, the height of this barrier is only 10 meV as opposed to something of order 200 meV in the depletion model. Furthermore, the potential change reduces to zero within three to four layers. This means that the size of our unit cell (20 layers) is in fact large enough to capture the effect. Making the cell larger will not significantly change the results. It means that the local charge density right next to the SF is even higher than estimated above (of order $10^{21}e/\mathrm{cm}^3$) and thus very significant metallic-type screening occurs, rather than only dielectric screening as assumed by the depletion model. A similar effect was recently noticed for self-consistent calculations of electrons in a triangular potential well in an entirely different system of perovskite interfaces.[31]

The bottom line is that when screening is included self-consistently, the effects of the potential barrier proposed by Kuhr *et al.*[14] become negligible. Thus an electronic driving force becomes a possibility again even for the SSF. Nevertheless, the driving force is much smaller for a SSF than for a DSF. This could explain why in the annealing situation, which presumably achieves thermodynamic equilibrium, one finds almost exclusively DSFs. Furthermore, one might argue that in the annealing situation the driving force for a SSF is so marginally small (of order a few meV/SiC pair) that it is not likely for SSF to form. On the other hand, in the device in operation, or in the presence of laser excitation, one could think of there being a local increase in electron density, and hence an increased dynamic quasi-Fermi energy. Clearly, according to Eq. (3) if E_F goes up, the driving force will increase as well.

IV. CONCLUSION

In conclusion, we have re-examined the driving force for growth of SFs in 4*H*-SiC in terms of an electronic model in which the energy cost for creating the additional SF area is offset by energy gain from capturing electrons in an interface localized state below the conduction band and found it to be an order of magnitude larger for a DSF than for SF in 4*H*-SiC. Screening significantly reduces the potential barrier adjacent to the quantum well and makes its effect negligible. The electron driving force, which was already well established for DSF thus appears to be at least a possible explanation for SSF expansion. Although its net energy gain, of order a few meV/SiC unit, is quite small under equilibrium conditions, it is found to be positive and, furthermore, it may be enhanced by a dynamically enhanced quasi-Fermi level in the presence of current.

ACKNOWLEDGMENTS

This work was supported by the Office of Naval Research. The calculations were performed on the Beowulf AMD cluster at the Ohio Supercomputing Center (OSC) under Project No. PDS0145. The authors thank P. Pirouz and M. Skowronski for useful discussions.

[1] J. P. Bergman, H. Lendenmann, P. Å. Nilsson, U. Lindefelt, and P. Skytt, in *Silicon Carbide and Related Materials*, Proceedings of the European Conference on Silicon Carbide and Related Materials, ECSCRM-2000 [Mater. Sci. Forum **353-3**, 299 (2000)].

[2] R. E. Stahlbush, J. B. Fedison, S. D. Arthur, L. B. Rowland, J. W. Kretchmer, and S. Wang, Mater. Sci. Forum **389**, 427 (2002).

[3] R. S. Okojie, M. Zhang, P. Pirouz, S. Tumakha, G. Jessen, and L. Brillson, Appl. Phys. Lett. **79**, 3056 (2001).

[4] L. J. Brillson, S. Tumakha, G. H. Jessen, R. S. Okojie, M. Zhang, and P. Pirouz, Appl. Phys. Lett. **81**, 2785 (2002).

[5] J. Q. Liu, H. J. Chung, T. Kuhr, Q. Li, and M. Skowronski, Appl. Phys. Lett. **80**, 2111 (2002).

[6] M. S. Miao, S. Limpijumnong, and W. R. L. Lambrecht, Appl. Phys. Lett. **79**, 4360 (2001).

[7] H. P. Iwata, U. Lindefelt, S. Öberg, and P. R. Briddon, Mater. Sci. Forum **389-393**, 529 (2002); J. Phys.: Condens. Matter **14**, 12733 (2002); Phys. Rev. B **65**, 033203 (2002); **68**, 113202 (2003).

[8] H. Iwata, U. Lindefelt, S. Öberg, and P. R. Briddon, J. Appl. Phys. **93**, 1577 (2003).

[9] H. Iwata, U. Lindefelt, S. Öberg, and P. R. Briddon, Microelectron. J. **34**, 371 (2003); Phys. Rev. B **68**, 245309 (2003).

[10] U. Lindefelt, H. Iwata, S. Öberg, and P. R. Briddon, Phys. Rev. B **67**, 155204 (2003).

[11] P. Pirouz, M. Zhang, J-L. Demenet, and H. M. Hobgood, J. Phys.: Condens. Matter **14**, 12929 (2002); J. Appl. Phys. **93**, 3279 (2003); P. Pirouz, J. L. Demenet, and M. H. Hong, Philos. Mag. A **81**, 1207 (2001).

[12] S. Ha, M. Skowronski, J. J. Sumakeris, M. J. Paisley, and M. K. Das, Phys. Rev. Lett. **92**, 175504 (2004).

[13] H. J. Chung, J. Q. Liu, and M. Skowronski, Appl. Phys. Lett. **81**, 3759 (2002).

[14] T. A. Kuhr, J. Q. Liu, H. J. Chung, M. Skowronski, and F. Szmulowicz, J. Appl. Phys. **92**, 5863 (2002).

[15] T. Miyanagi, H. Tsuchida, I. Kamata, T. Nakamura, R. Ishii, K. Nakayam, and Y. Sugawara, in Proceedings of International Conference on Silicon Carbide and Related Materials, 2005 [Mater. Sci. Forum (to be published)].

[16] P. K. Sitch, R. Jones, S. Öberg, and M. I. Heggie, Phys. Rev. B **52**, 4951 (1995).

[17] A. T. Blumenau, C. J. Fall, R. Jones, S. Öberg, T. Frauenheim, and P. R. Briddon, Phys. Rev. B **68**, 174108 (2003); A. T. Blumenau, C. J. Fall, R. Jones, M. I. Heggie, P. R. Briddon, T. Frauenheimn, and S. Oberg, J. Phys.: Condens. Matter **14**, 12749 (2002).

[18] A. Galeckas, J. Linnros, and P. Pirouz, Appl. Phys. Lett. **81**, 883 (2002).

[19] M. S. Miao and W. R. L. Lambrecht, in Proceedings of Interna-

tional Conference on Silicon Carbide and Related Materials, 2005, edited by R. P. Devaty, D. Larkins, and S. Saddow [Mater. Sci. Forum (to be published)].

[20] M. Methfessel, M. van Schilfgaarde, and R. A. Casali, in *Electronic Structure and Physical Properties of Solids, The Uses of the LMTO Method*, edited by Hugues Dreyssé, Springer Lecture Notes, Workshop Mont Saint Odille, France, 1998 (Springer, Berlin, 2000), pp. 114–147.

[21] E. Bott, M. Methfessel, W. Krabs, and P. C. Schmidt, J. Math. Phys. **39**, 3393 (1998).

[22] S. Limpijumnong and W. R. L. Lambrecht, Phys. Rev. B **57**, 12017 (1998).

[23] L. Hedin and B. I. Lundqvist, J. Phys. C **4**, 2064 (1971).

[24] P. Hohenberg and W. Kohn, Phys. Rev. **136**, B864 (1964); W. Kohn and L. J. Sham, Phys. Rev. **140**, A1133 (1965).

[25] M. E. Fisher and W. Selke, Phys. Rev. Lett. **44**, 1502 (1980).

[26] C. Cheng, R. J. Needs, V. Heine, and N. Churcher, Europhys. Lett. **3**, 475 (1987).

[27] W. R. L. Lambrecht and B. Segall, Phys. Rev. B **52**, R2249 (1995).

[28] A. Qteish, V. Heine, and R. J. Needs, Phys. Rev. B **45**, 6534 (1992); **45**, 6376 (1992).

[29] M. S. Miao and W. R. L. Lambrecht, Phys. Rev. B **68**, 155320 (2003).

[30] M. S. Miao and W. R. L. Lambrecht (unpublished).

[31] Z. S. Popovic and S. Satpathy, Phys. Rev. Lett. **94**, 176805 (2005).